Journal of Applied Research in Science and Humanities

Metal oxide semiconductors for water remediation application

Hagar Ashraf Abdel Moneim, Hala Mahmoud Abdelsamee, Hayam Ramadan Abou El-Ela, Walaa Nabil Said and Yara Mohamed Abdel Moghny

Supervisor: Hanan Atef Soliman, Lecturer of physical chemistry

Ain Shams University, Faculty of Education, Bachelor of Science and Education (preparatory and secondary), specializing in Chemistry

Abstract

The $ZnO/CuO/ZnFe_2O_4$ nanocomposite was successfully synthesized using the co-precipitation method and subjected to calcination at 800°C for 3 hours. The formation of the nanocomposite was confirmed through X-ray powder diffraction (XRD), while its optical properties were evaluated using UV-Vis diffuse reflectance spectroscopy. XRD analysis identified the presence of ZnO, $ZnFe_2O_4$, and CuO phases, which correspond to JCPDS cards 36–1451, 22–1012, and 45–0937, respectively, with an estimated crystal size of 30.58 nm. The UV-Vis diffuse reflectance spectrum demonstrated that the synthesized nanocomposite effectively absorbed both ultraviolet and visible light, exhibiting band gap energy of 1.87 eV. Furthermore, 0.1 g of the co-precipitated $ZnO/CuO/ZnFe_2O_4$ nanocomposite was applied in the photo-Fenton catalytic decolorization of a 50 mL remazol red solution (1.6×10^{-5} M) in the presence of 3% H_2O_2, achieving an apparent rate constant of 0.005 min^{-1} and a decolorization efficiency of 79.5%.

Key Words:

Photo-Fenton - ZnO - $ZnFe_2O_4$ - CuO – Co-precipitation - Remazol Red

1. Introduction:

One of the serious global challenges facing humanity in this era is providing a sustainable source of clean water. Many factors affect water quality, such as industrial and agricultural waste, which contain highly toxic pollutants like dyes and other organic compounds. Since water is essential for human life, its pollution is a major problem that requires urgent action and effective solutions (Abdel-Raouf et al., 2019, 018-034). Photo-oxidation technologies are among the most promising and effective methods for water purification. They rely on the power of ultraviolet light from sunlight to oxidize and reduce pollutants in different environments (Iyyappan et al., 2024, 100599-100615).

The essence of these methods lies in the absorption of sunlight or UV light by contaminated water in the presence of an oxidant and catalyst, which helps generate reactive oxidizing species that break down pollutants into non-toxic molecules such as water, carbon dioxide, and inorganic salts. Examples of these oxidants include hydrogen peroxide, ozone, and persulfate, which in turn produce reactive oxidizing species under the influence of various solar radiation components.

These methods offer several advantages, such as easy process control, harmless byproducts, no need for off-gas treatment, and no requirement for multiple treatment stages, in addition to the complete removal of pollutants (Iyyappan et al., 2024, 100599-100615; Khader et al., 2024, 100384-100398).

The effectiveness of the photo-oxidation process depends on the oxidizing agent involved. One of the important oxidants is the hydroxyl radical due to its characteristics, such as high reactivity, strong oxidizing power, easy generation, short lifespan, and harmless nature (Sharma et al., 2020, 221-255). They are produced through various processes such hydrogen peroxide/ultraviolet photolysis (H_2O_2/UV) that involves photolysis and oxidation simultaneous reactions. UV light cleaves H_2O_2 to form of hydroxyl radicals. $H_2O_2 + h\upsilon \rightarrow 2\ ^{\bullet}OH$. These radicals interact with organic compounds in water, generating organic radicals that subsequently react with dissolved oxygen to form hydroperoxyl radicals. These newly formed radicals then trigger oxidation reactions, breaking down contaminants into smaller, harmless fragments (Khader et al., 2024, 100384-100398).

Another process is photolytic ozonation (UV/O_3), where O_3 is a powerful oxidant for organic and inorganic pollutants that produce hydroxyl radicals and others through several reactions (Khader et al., 2024, 100384-100398). Photocatalysis is another technique used to treat contaminant water through producing radicals. In which a photocatalyst (such as TiO_2) is illuminated with energy exceeding its optical band gap, its molecules absorb the energy, causing an electron to move to the conduction band and leaving a hole in the valence band. This electron can either transfer to an acceptor in the solution or be replaced by a donor transferring electrons to the valence band at the solid–liquid interface. Without effective electron and hole trappers, the stored energy disperses due to recombination. The holes in the valence band act as strong oxidants that interact with H_2O to produce $^{\bullet}OH$ hydroxyl radical, while the conduction band electrons serve as effective reductants which interact with surface adsorbed O_2 to give $O_2^{-\bullet}$ superoxide radical anions. Those radicals contribute to the breakdown of organic contaminants (Chakravorty & Roy, 2024, 100155-100173; Ikram et al., 2021, e00343-e00385).

Additionally, $^{\bullet}OH$ radicals can be produced through the homogeneous Fenton reaction – based process in which Fe^{2+} salts react with H_2O_2 (Fenton process; Fe^{2+}/H_2O_2; $Fe^{2+} + H_2O_2 \rightarrow Fe^{3+} + OH^- + {}^{\bullet}OH$) or through Fenton-like process when M^{n+} compounds interact with H_2O_2 ($M^{n+} = Fe^{3+}$, Co^{2+}, Mn^{2+}, and Cu^{2+}/ H_2O_2) (Das & Adak, 2022, 100282-100302; Machado et al., 2023, 13995–14032; Vorontsov, 2019, 103-112).

Also, there is heterogeneous Fenton-like reaction that involves the interaction of hydrogen peroxide (H_2O_2) with solid compounds containing iron, such as iron oxides, and others. The heterogeneous nature of this reaction allows it to occur at any pH level, in addition to being easy to handle with the possibility of recycling. To maximize the benefit of pollutant degradation through exposure to UV and visible light and the Fenton reaction, the photo-Fenton technique emerges to be effective than Fenton process. Through this reaction hydroxyl radical and others are formed and undergo to degrade the water contaminate according to the following steps (Figure 1): (Machado et al., 2023, 13995–14032; Ribeiro et al., 2024, 591-609; Vorontsov, 2019, 103-112)

$Fe^{3+} + h\upsilon \rightarrow Fe^{2+} + {}^{\bullet}OH$

$H_2O_2 + h\upsilon \rightarrow 2\ {}^{\bullet}OH$

$RH + {}^{\bullet}OH \rightarrow H_2O + R^{\bullet}$

$R^{\bullet} + H_2O_2 \rightarrow ROH + {}^{\bullet}OH$

$R^{\bullet} + O_2 \rightarrow ROO^{\bullet}$

The target of our study is to discard remazole red dye from textile waste water through photo-Fenton process using ternary composite photocatalyst. The removal of this dye using $ZnO/CuO/ZnFe_2O_4$ nanocomposite through photo-Fenton technology is not recorded yet.

2. The Theoretical Framework

Semiconductor photocatalysts have been widely applied in photo-Fenton process due to their optical and catalytic properties. Zinc oxide is considered to be one of those photocatalysts that has high photocatalytic activity in spite of its limiting application in visible light due to its broad band gap. Combing ZnO with other semiconductors can enhance its photocatalytic activity based on the charge transfer between them that effectively separate the photogenerated electrons and holes. Zinc ferrite ($ZnFe_2O_4$) and copper oxide (CuO) are semiconductors can be used to expand the ability of ZnO to absorb visible light rang due to their narrow band gaps. The ternary $ZnO/CuO/ZnFe_2O_4$ nanocomposite has a great photocatalytic activity compared to the physical mixed of three oxides due to the formation of ${}^{\bullet}OH$ radicals (Bi et al., 2024, 111066-111075).

Synthesizing the ternary nanocomposite from ZnO, CuO, and $ZnFe_2O_4$ is limited in the literature, and the following presents a review of the existing studies.

Li et al., 2018, prepared the $ZnO/CuO/ZnFe_2O_4$ nanocomposite by co-precipitating Zn^{2+}, $Cu^{2+}$and Fe^{3+} from their salts and tested different the calcination temperature to reach the suitable temperature for ternary composite preparation. Then they characterized the composite with different tools. The photocatalytic activity of the $ZnO/CuO/ZnFe_2O_4$ nanocomposite as a photoFenton-like catalyt was examined under ultraviolet (UV), visible (Vis) and near-infrared (NIR) for methyl orange degradation.

Al-Gaashani et al., 2019, used a one-step thermal decomposition method to prepare ZnO-CuO-$ZnFe_2O_4$ nanocomposite from salts of Zn, Cu and Fe as precursors at two different temperatures (400 and 500 °C). The crystal structure, the elemental compositions, the morphology, the thermal stability and the light absorption of prepared nanocomposites were examined by X-ray diffraction, X-ray photoelectron spectroscopy, scanning electron microscope with energy dispersive X-ray spectroscopy, thermogravimetric analysis and UV–Vis diffuse reflectance spectroscopy, respectively.

Bi et al., 2024, synthesized photo-Fenton nanofiber of $ZnFe_2O_4$/ZnO/CuO composite by electrospinning technique and characterized by X-ray diffraction, X-ray photoelectron spectroscopy, transmission electron microscopy, electron spin resonance, ultraviolet-visible diffuse reflectance spectroscopy and fluorescence spectroscopy. The photocatalytic of the $ZnFe_2O_4$/ZnO/CuO photo-Fenton like catalyst was evaluated by the degradation of Rhodamine B.

Our study focuses on synthesizing ZnO/CuO/$ZnFe_2O_4$ nanocomposite using co-precipitation method, characterizing its chemical structure and optical properties by XRD and UV-Vis diffuse reflectance to employ it as a photo-Fenton like catalyst for remazole red decolorizing.

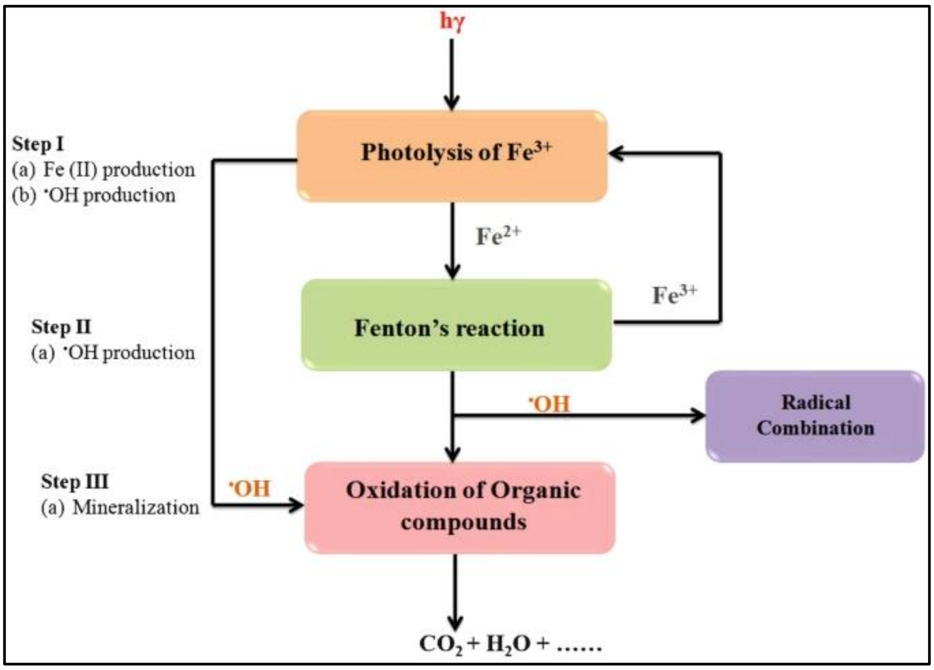

Figure (1): Schematic representation of photo-Fenton pathway (Sharma et al., 2020, 221–255)

3. Methods of Research and the tools used

3.1. Chemicals and equipment

The chemicals utilized in this work include zinc nitrate hexahydrate ($Zn(NO_3)_2.6H_2O$) from WINLAB, cupric nitrate trihydrate ($Cu(NO_3)_2.3H_2O$) from Oxford and Ferric nitrate nonahydrate ($Fe(NO_3)_3.9H_2O$) from LOBA CHEMIE; nitrate salts were stored in a desiccator. Remazol Red RB-133 with molecular structure illustrated in Figure 2 was obtained from DyeStar. Sodium hydroxide (ALPHA AROMATIC), sodium carbonate anhydrous (Biotech), 3% hydrogen peroxide (from a local market) and deionized water were also used. The equipment used for nanocomposite preparation is listed in Table 1.

3.2. PhotoFenton–like ZnO/ CuO/ $ZnFe_2O_4$ nanocomposite's synthesis

The ZnO/ CuO/ $ZnFe_2O_4$ nanocomposite was synthesized using co-precipitation method (Li et al., 2018, 557-569). 1.34 g of zinc nitrate hexahydrate (0.045 M), 0.36 g of cupric nitrate trihydrate (0.015 M) and 0.81 g of ferric nitrate nonahydrate (0.02 M) were homogeneously mixed together in a total volume of 100 mL deionized water. In 100 mL deionized water; 1.40 g of sodium carbonate (0.35 M) was mixed with 0.53 g of sodium hydroxide (0.05 M) to prepare a mixed alkali aqueous solution. The mixed alkali solution was gradually added to the previously prepared mixed nitrate salt solution under vigorous stirring until the pH of that solution reached 10.5. The resultant slurry was continuously stirred for half an hour and then aged for three hours (3 h) at 65°C. The slurry was centrifugally separated and washed repeatedly with deionized water. After that it was dried in a furnace at 80°C for 24 hours. Finally the dried solid was ground and calcined at 800°C for three hours to obtain a black powder. A schematic representation of ZnO/ CuO/ $ZnFe_2O_4$ nanocomposite's synthesis process is shown in Figure 3.

3.3. Monitoring of PhotoFenton–like Catalytic activity

The photofenton–like catalytic activity of ZnO/ CuO/ $ZnFe_2O_4$ nanocomposite was examined by evaluating its effect on the decolourization of an aqueous remazol red solution in the presence of H_2O_2 under simulated solar light source using a 500 W Xe lamp. Approximately 0.1 g of ZnO/ CuO/ $ZnFe_2O_4$ nanocomposite was vigorously stirred with 50 mL of 3% H_2O_2 containing remazol red ($1.6x10^{-5}$M) in darkness for 30 minutes to reach adsorption/desorption equilibrium. Under continuous stirring, the solution was exposed to light source and every 20 minutes, a small portion the sample was taken and centrifuged at 7000 rpm for 30 minutes to remove the fine particles of catalyst while the UV-vis absorption of the dye was measured using a UV–vis spectrophotometer.

3.4. Characterization of prepared photo–Fenton like catalyst

The ZnO/ CuO/ $ZnFe_2O_4$ nanocomposite's chemical structure and optical properties were examined through X- ray powder diffraction and UV–vis diffuse reflectance techniques, respectively. The used equipment model were listed in Table 2

Table 1: Preparation equipment.

Equipment	Model
Magnetic stirrer with hot plate	JENWAY 1000 magnetic stirrer (100-1000 r/min) with hot plate
pH Meter	JANWAY 3505 ion analyzer
Centrifuge	Centrifuge model ECCO-LABOR-1 of a maximum speed 9000 RPM

Equipment	Model
Oven	HST 5020
Muffle furnace	VULCAN® A-550 Ney® muffle furnace

Table 2: **Characterization equipment**.

Measured technique	Equipment model
X-ray powder diffraction (XRD)	Bruker D8 Advance X-ray diffractometer with Cu Kα radiation at 10 kV and 10 mA.
UV–vis diffuse reflectance (DR)	JASCO V-530" spectrometer with $BaSO_4$ reference.

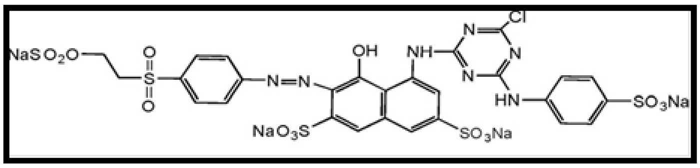

Figure (2). **Ramazol Red structure** (**Pavithra**, **2017**, **247–255**)

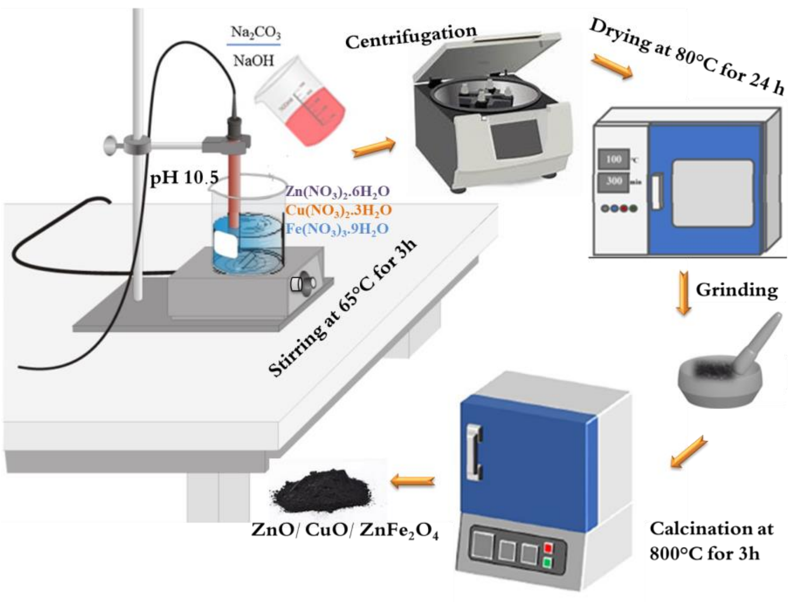

Figure (3). **ZnO/ CuO/ $ZnFe_2O_4$ nanocomposite's synthesis**

4. Results of Research

4.1. XRD

The crystallographic structure and crystallite size of the prepared photoFenton-like ZnO/ CuO/ $ZnFe_2O_4$ catalyst were examined using X-ray diffraction (XRD) analysis. Figure 4 explores its XRD pattern. At the calcination temperature 800 °C, the diffraction peaks belongs to hexagonal ZnO phase, monoclinic CuO phase and the spinel cubic $ZnFe_2O_4$ phase are appeared and matched with JCPDS cards no. 36–1451, 45–0937 and 22–1012, respectively. For hexagonal ZnO, the diffraction peaks are found at 31.87°, 34.65°, 36.70°, 47.81°, 56.89°, 63.02°,66.35°, 68.21° and 69.33° (2θ) angles. While CuO phase appears at 2θ = 35.40°, 39.11° and 48.92°. The diffraction peaks of $ZnFe_2O_4$ phase are 18.52°, 30.20°, 35.40°, 37.24°, 43.18°, 53.37°, 56.89°and 62.45°. The diffraction peaks are slightly shifted to higher angle (Li et al., 2018, 557-569).

The calculated crystalline size (L) is 305.8 Å (30.58 nm) based on the application of the Scherrer equation [L = (0.9 * λ)/(β * cos θ); where λ = 1.5406 Å (for Cu Kα radiation), β is the full width at half maximum (FWHM in radians), and θ is the diffraction angle (in degrees)] to the highest intensity peak (Hassanzadeh-Tabrizi, 2023, 171914-171934).

4.2. UV-Vis diffuse reflectance

The UV-Vis diffuse reflectance (DR) of ZnO/ CuO/ $ZnFe_2O_4$ nanocomposite calcined at 800°C/3h was examined, resulting in the spectrum shown in Figure 5 (a) and optical data collected in Table 3. From the intended spectrum, a broad absorption band ranged from 200 to 700nm was found with an absorption edge appearing at 664.11nm. Which emphasized that ZnO/ CuO/ $ZnFe_2O_4$ photo-Fenton nanocomposite could absorb ultraviolet light and visible light. ZnO/ CuO/ $ZnFe_2O_4$ nanocomposite's band gap value (E_g) was calculated using the Wood and Tauc equation (Soliman, 2023, 7280-7295);

$$\alpha\, h\upsilon = constant\ (h\upsilon - E_g)^m$$

by plotting $(\alpha h\upsilon)^2$ as a function of hυ. In this context, the absorption coefficient (α) is given by the equation: α = 2.303 x $\ln(I_o/I)/t$, where $\ln(I_0/I)$, t and hυ represent the absorbance, the sample thickness and the photon energy of the incident radiation, respectively. The parameter m characterizes the optical transition type, with m=0.5 for direct allowed transitions and m=2 for indirect allowed transitions. It was found that the calculated band gap equal to be 1.87 eV (Figure 5(b)).

Table 3: ZnO/ CuO/ $ZnFe_2O_4$'s optical parameters obtained from UV-Vis DR .

Sample	Absorption edge (nm)	Band gap (eV)
ZnO/ CuO/ $ZnFe_2O_4$	664.11	1.87

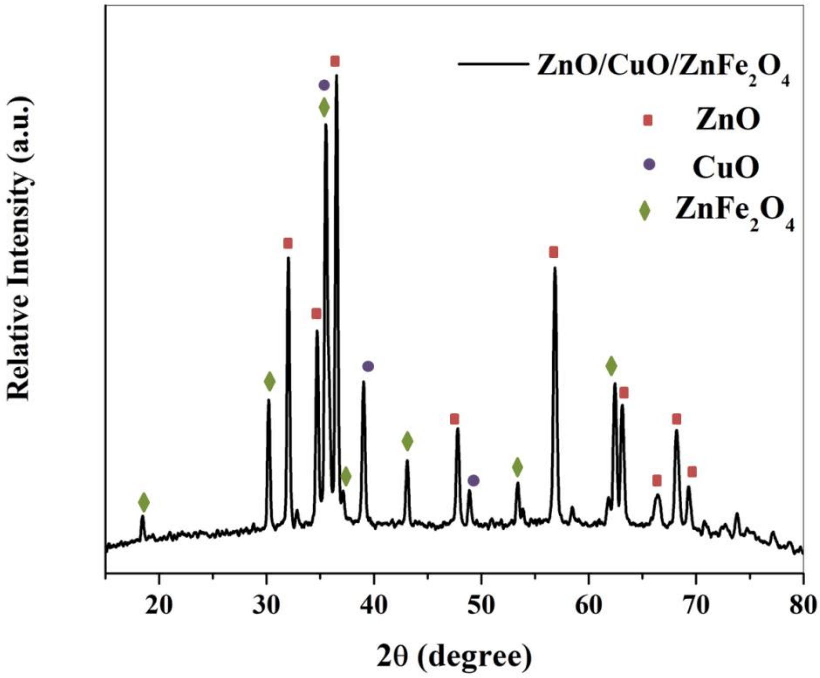

Figure (4): XRD pattern of ZnO/ CuO/ $ZnFe_2O_4$

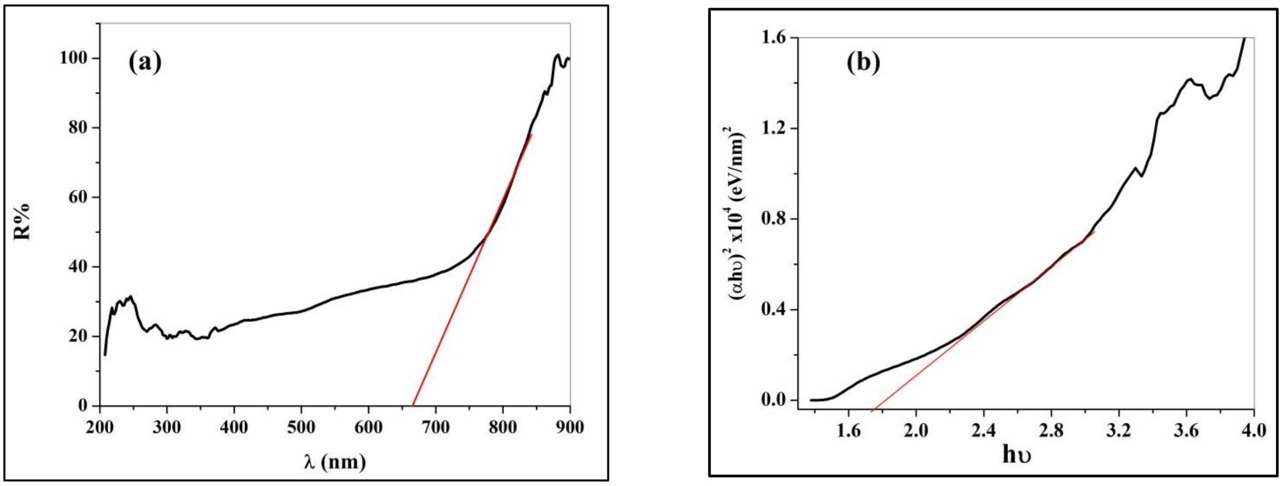

Figure (5): (a) UV– vis/DR spectrum of ZnO/ CuO/ $ZnFe_2O_4$ and (b) $(\alpha h\upsilon)^2$ vs. photon energy (hν).

4.3. PhotoFenton–like Catalytic Activity of ZnO/ CuO/ $ZnFe_2O_4$

The target contaminant used to examine the photofenton-like catalytic capability of ZnO/ CuO/ $ZnFe_2O_4$ nanocomposite was Remazol Red RB-133. The capability of ZnO/ CuO/ $ZnFe_2O_4$ nanocomposite to decolorize the remazol red dye's solution was monitored by measuring its absorbance spectra for 5 hours under simulated solar illumination at 25°C. The remazol red's absorbance spectra were examined from 430 to 600 nm under illumination time as shown in Figure 6, in which the absorbance peak of remazol red dye at 525 nm was decreased gradually. That indicates the dye molecule's decolorization. After 5 hours of illumination, the dcolorization efficiency (%D) of remazol red equal 79.5% with correlation factor (R) = 0.98.

Decolorization efficiency (%D) formula that was applied at 525 nm is: (Ara et al., 2013, 93-98):

$$\%D = \frac{C_o - C_t}{C_o} \times 100 = \frac{A_o - A_t}{A_o} \times 100$$

Here, A_0 denotes represents the initial absorbance of remazol red (corresponding to its initial concentration C_0), while A_t represents the absorbance at a specific time interval t (corresponding to the concentration C_t).

The decolorization kinetics of remazol red dye was analyzed by calculating the reaction rate constant using a pseudo-first-order model, as expressed in the following equation (Elkahoui et al., 2025, 23-51).

$$\ln\left(\frac{A_t}{A_o}\right) = -k_{app}t$$

The apparent rate constant k_{app} is the slop of $\ln(A_t / A_o)$ versus time (t) plot to be 0.005 min^{-1} (Figure 7). The observed apparent rate constant (k_{app}, min^{-1}) of ZnO/ CuO/ $ZnFe_2O_4$ nanocomposite as well as its specific rate constant (K, min^{-1} g^{-1}) were listed in Table 4.

The degradation ability of ZnO/ CuO/ $ZnFe_2O_4$ is also found to be negligible in the absence of irradiation, as seen in Figure (8) and in the absence of H_2O_2, as shown in Figure (9), indicating that the reaction is a typical photoFenton reaction.

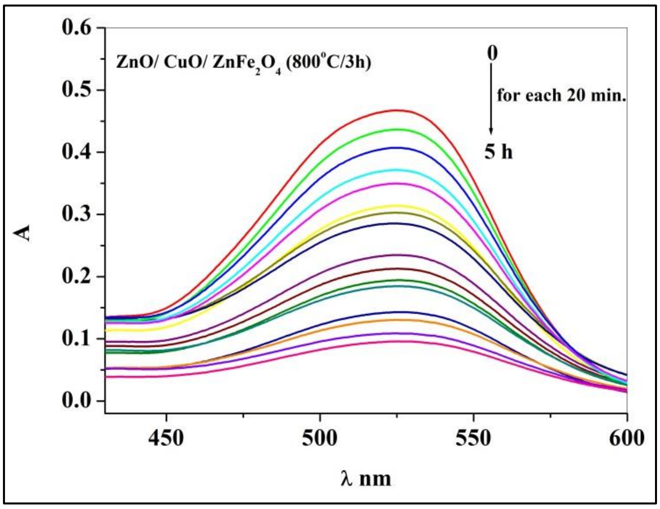

Figure (6): Absorbance spectra of remazol red the under simulated solar irradiation in the presence of ZnO/ CuO/ $ZnFe_2O_4$.

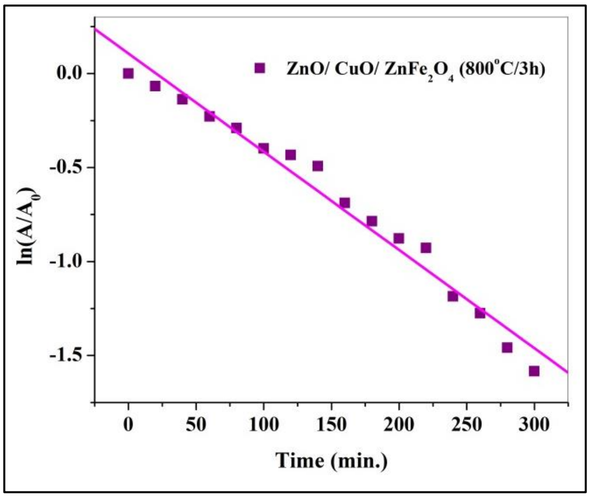

Figure (7): Dye's Decolorization Rate in the presence ZnO/ CuO/ $ZnFe_2O_4$.

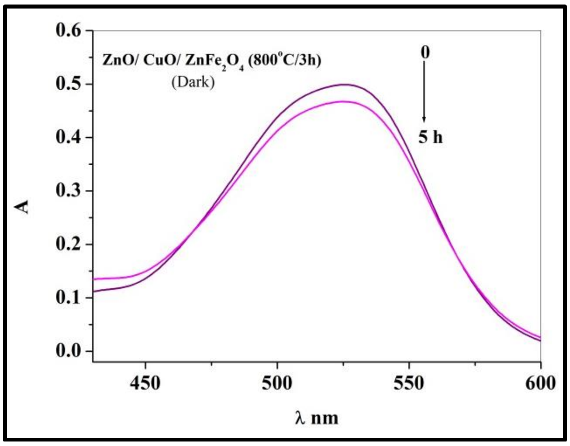

Figure (8): Absorbance spectra of remazol red without irradiation in the presence of ZnO/ CuO/ $ZnFe_2O_4$.

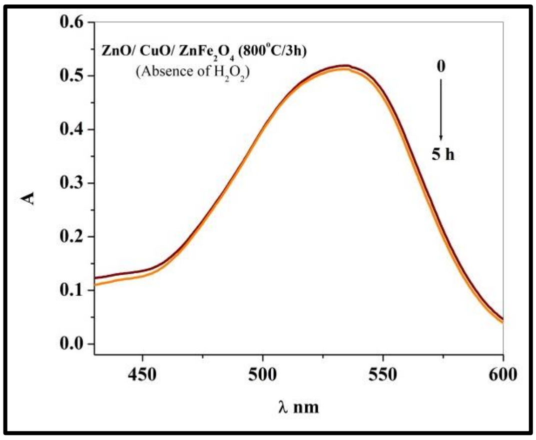

Figure (9): Absorbance spectra of remazol red without H_2O_2 in the presence of ZnO/ CuO/ $ZnFe_2O_4$.

Taple (4): kinetic parameters of remazol red decolorization by ZnO/ CuO/ $ZnFe_2O_4$

Sample	**K_{app} min^{-1}**	**R**	**K (min^{-1}g^{-1})**	**Decolorization %**
ZnO/ CuO/ $ZnFe_2O_4$	0.005	0.98	0.05	79.5

5. Interpretation of Results

From the previously mentioned data in the above sections, ZnO/ CuO/ $ZnFe_2O_4$ nanocomposite was perfectly prepared using co-precipitation method according to XRD pattern. And depending on the UV-Vis DR spectra, there is the strong synergistic effect between ZnO, CuO and $ZnFe_2O_4$ that absorb ultraviolet light and visible light. In addition to the previously reported studies (Al-Gaashani et al., 2019, 41-49; Bi et al., 2024, 111066-111075; Li et al., 2018, 557-569) that proved the photofenton catalytic ability of ZnO/ CuO/ $ZnFe_2O_4$ to degrade the organic dyes. We propose the photofenton mechanism of remazol red removal via ZnO/ CuO/ $ZnFe_2O_4$ (Figure 10). After the adsorption/desorption equilibrium of remazol red on the surface of as-prepared nanocomposite was reached, the system was illuminated by simulated solar source. The nanocomposite absorbed the energy of the bandgap (E_g) of its components and the electrons/holes were formed; the electrons transferred to the conduction band (CB), leaving holes in the valence band (VB). Due to the strong synergistic effect between ZnO, CuO and $ZnFe_2O_4$, the photoinduced e^-/h^+ pairs are perfectly separated.

$$ZnO \overset{h\upsilon}{\rightarrow} h^+ + e^-$$

$$CuO \overset{h\upsilon}{\rightarrow} h^+ + e^-$$

$$ZnFe_2O_4 \overset{h\upsilon}{\rightarrow} h^+ + e^-$$

As a result, the photoinduced charge carriers undergo different reactions. The conduction band electrons may interact with either the adsorbed oxygen on the surface forming of superoxide radicals ($O_2^{-\bullet}$)

$O_2 + 2e^- \rightarrow O_2^{-\bullet}$

or with H_2O_2 forming $^{\bullet}OH$.

$H_2O_2 + e^- \rightarrow OH^- + {}^{\bullet}OH$

As well as, the electrons play vital role in reduction/oxidation cycles of both Fe^{3+}/Fe^{2+} and Cu^{2+}/Cu^{+} of the composite. Fe^{3+} and Cu^{2+} are electron trappers and could be reduced to Fe^{2+} and Cu^{+}, respectively. Fe^{2+} and Cu^{+} subsequently react with H_2O_2 to generate more $^{\bullet}OH$ radicals and are reoxidized again to $Fe^{3+}$and Cu^{2+}.

$Fe^{3+} + e^- \rightarrow Fe^{2+} \xrightarrow{H_2O_2} Fe^{3+} + OH^- + {}^{\bullet}OH$

$Cu^{2+} + e^- \rightarrow Cu^{+} \xrightarrow{H_2O_2} Cu^{2+} + OH^- + {}^{\bullet}OH$

Also photogenerated holes can react with H_2O or with OH^- forming $^{\bullet}OH$

$H_2O + h^+ \rightarrow H^+ + {}^{\bullet}OH$

$OH^- + h^+ \rightarrow {}^{\bullet}OH$

The reactive hydroxyl and superoxide radicals ($OH^{\bullet}$ and $O_2^{-\bullet}$) oxidize the adsorbed remazol red molecules on the nanocomposite's surface and give non-toxic byproducts.

$OH^{\bullet}$ / $O_2^{-\bullet}$ + Dye $\rightarrow CO_2 + H_2O +$ degradation product

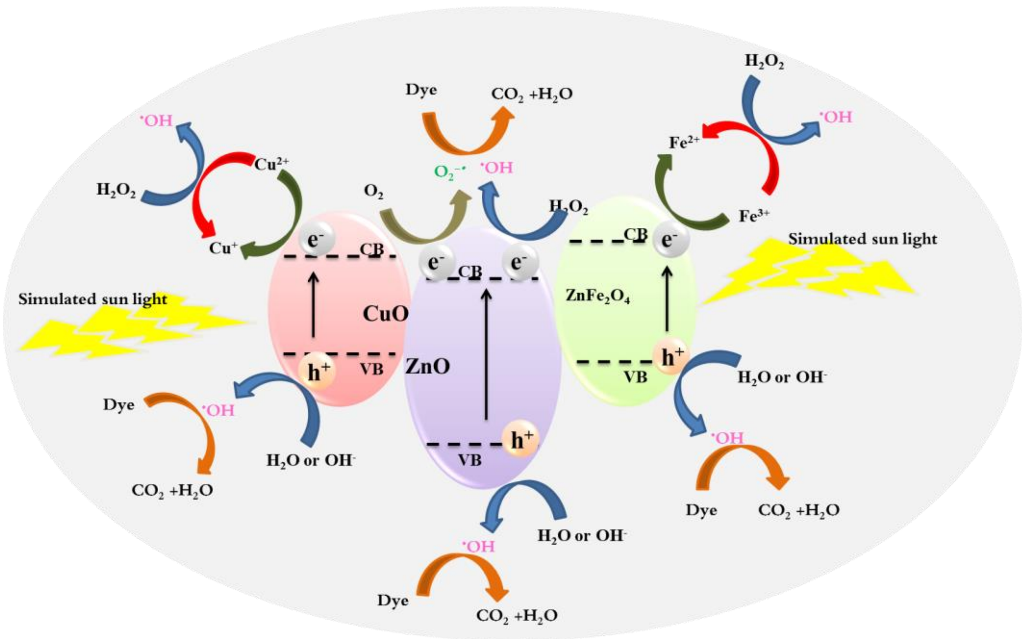

Figure (10): Proposed dye's decolorization mechanism using ZnO/ CuO/ $ZnFe_2O_4$.

6. Conclusion

The ZnO/CuO/$ZnFe_2O_4$ nanocomposite was successfully co-precipitated and calcined at 800°C for 3 hours. Then its formation was confirmed by X-ray powder diffraction (XRD), and its optical properties were determined from UV-Vis diffuse reflectance measurements. XRD analysis revealed the presence of three phases: ZnO, $ZnFe_2O_4$, and CuO, which correspond to JCPDS cards 36–1451, 22–1012, and 45–0937, respectively, with an average crystal size of 30.58 nm. The UV-Vis diffuse reflectance spectrum confirmed that the prepared nanocomposite absorbed both ultraviolet and visible light, exhibiting band gap energy of 1.87 eV.

In this study, 0.1 g of the co-precipitated $ZnO/CuO/ZnFe_2O_4$ nanocomposite was successfully applied in the photo-Fenton catalytic decolorization of an aqueous solution containing 50 mL of remazol red dye at a concentration of 1.6×10^{-5} M. The experiment was conducted in the presence of 3% hydrogen peroxide (H_2O_2) to enhance the generation of hydroxyl radicals ($^{\bullet}OH$). The catalytic reaction was monitored over time, and the results demonstrated that the process has an apparent rate constant of 0.005 min^{-1} with a moderately high decolorization efficiency of 79.5%, indicating the effective removal of synthetic dyes from wastewater. These findings suggest that the $ZnO/CuO/ZnFe_2O_4$ nanocomposite can serve as an effective photo-Fenton like catalyst in advanced oxidation processes.

Based on the data obtained and the recorded results, we recommend further examinations to gain more insights into the prepared nanocomposite. This includes using scanning electron microscopy (SEM) and transmission electron microscopy (TEM) for a deeper understanding of its morphology, as well as measuring the specific surface area and pore size distribution due to their significant impact on its photocatalytic activity. Additionally, the Chemical Oxygen Demand (COD) and Total Organic Carbon (TOC) can be measured to ensure the complete photocatalytic degradation of the dye. Furthermore, the effect of catalyst dosage, hydrogen peroxide concentration, dye concentration, and the pH of the dye solution can be studied due to their influence on the decolorization efficiency.

Acknowledgement

We sincerely appreciate the support of our supervisor at the Physical and Inorganic Chemistry Research Laboratories, Department of Chemistry, Faculty of Education, Ain Shams University, for granting us access to essential preparation and characterization equipment. Our deepest gratitude goes to Professor Dr. Mona Mustafa Saif, Professor of Inorganic Chemistry, for authorizing the use of the JASCO V-530 device for UV-Vis Diffuse Reflection measurements. Additionally, we extend our thanks to the Desert Research Center for their assistance in conducting the XRD measurements.

References and Sources

Abdel-Raouf, M. E., Maysour, N. E., Farag, R. K. & Abdul-Raheim, M. A. R. (2019). Wastewater treatment methodologies, review article. International Journal of Environment & Agricultural Science, 3, 018-034.

Al-Gaashani, R., Aïssa, B., Hossain, M. d. A., & Radiman, S. (2019). Catalyst-free synthesis of $ZnO-CuO-ZnFe_2O_4$ nanocomposites by a rapid one-step thermal decomposition approach. Materials Science in Semiconductor Processing, 90, 41-49.

Ara, N. J., Abu Hasan, M. d., Rahman, M. A., Salam, M. d. A., Salam, A. & Alam, A. M. S. (2013). Removal of Remazol Red from Textile Waste Water Using Treated

Sawdust – An Effective Way of Effluent Treatment. Bangladesh Pharmaceutical Journal, 16, 93-98.

Bi, F., Zhou, B., Li, R., Du, R., Zheng, Z., Fu, X., Zhao, L., Xiao, S., Wang, L. & Dong, X. (2024). One-step electrospun $ZnFe_2O_4$/ZnO/CuO composite photo-Fenton nanofibers for efficient degradation of organic dyes. Materials Today Communications, 41, 111066-111075.

Chakravorty, A. & Roy, S. (2024). A review of photocatalysis, basic principles, processes, and materials. Sustainable Chemistry for the Environment, 8, 100155- 100173.

Das, A. & Adak, M. K. (2022). Photo-catalyst for wastewater treatment: A review of modified Fenton, and their reaction kinetics. Applied Surface Science Advances, 11, 100282-100302.

Elkahoui, Y., Abahdou, F. Z., Ali, M. B., Alahiane, S., Elhabacha, M., Boutarba, Y. & El Hajjaji, S. (2025). Photocatalytic and Photo-Fenton-like Degradation of Cationic Dyes Using $SnFe_2O_4$/g-C_3N_4 Under LED Irradiation: Optimization by RSM-BBD and Artificial Neural Networks (ANNs). Reactions, 6, 23-51.

Hassanzadeh-Tabrizi, S.A. (2023). Precise calculation of crystallite size of nanomaterials: A review. Journal of Alloys and Compounds, 968, 171914-171934.

Ikram, M., Rashid, M., Haider, A., Naz, S., Haider, J., Raza, A., Ansar, M. T., Uddin, M. K., Ali, N. M., Ahmed, S. S., Imran, M., Dilpazir, S., Khan, Q. & Maqbool, M. (2021). A review of photocatalytic characterization, and environmental cleaning, of metal oxide nanostructured materials. Sustainable Materials and Technologies, 30, e00343-e00385.

Iyyappan, J., Gaddala, B., Gnanasekaran, R., Gopinath, M., Yuvaraj, D. & Kumar, V. (2024). Critical review on wastewater treatment using photo catalytic advanced oxidation process: Role of photocatalytic materials, reactor design and kinetics. Case Studies in Chemical and Environmental Engineering, 9, 100599-100615.

Khader, E. H., Muslim, S. A., Cata Saady, N. M., Ali, N. S., Salih, I. K., Mohammed, T. J., Albayati, T. M. & Zendehboudi, S. (2024). Recent advances in photocatalytic advanced oxidation processes for organic compound degradation: A review. Desalination and Water Treatment, 318, 100384-100398.

Li, Z., Chen, H. & Liu, W. (2018). Full-Spectrum Photocatalytic Activity of ZnO/CuO/$ZnFe_2O_4$ Nanocomposite as a PhotoFenton-Like Catalyst. Catalysts, 8, 557-569.

Machado, F., Teixeira, A. C. S. C. & Ruotolo, L. A. M. (2023). Critical review of Fenton and photo-Fenton wastewater treatment processes over the last two decades. International Journal of Environmental Science and Technology, 20, 13995–14032.

Pavithra, M. P. (2017). Electrochemical Oxidation of Dye by using Graphite and Titanium Based Electrodes. International Journal of Advances in Scientific Research and Engineering, 3, 247-255.

Ribeiro, J. A. S., Alves, J. F., Salgado, B. C. B., Oliveira, A. C., Araújo, R. S. & Rodríguez-Castellón, E. (2024).

Heterogeneous Photo-Fenton Degradation of Azo Dyes over a Magnetite-Based Catalyst: Kinetic and Thermodynamic Studies. Catalysts, 14, 591-609.

Sharma, R. K., Arora, B., Dutta, S. & Gawande, M. B. (2020). Photo-oxidation Technologies for Advanced Water Treatment. In J. Filip, P. Najmanová, R. Zbořil, T. Cajthaml & M. Černík (Ed.), Applied Environmental Science and Engineering for a Sustainable Future (pp. 221-255). Springer.

Soliman, H. A., Ali, L. I., Khaled, F. K., Hafez, H., Mbrouk, O. A., Saif, M. & Ibrahim, M. M. (2023). $Eu^{3+}:Y_2Ti_2O_7$ nanomaterials as efficient photocatalysts used for hydrogen and biogas production toward a sustainable environment. Applied Organometallic Chemistry, 37, 7280-7295.

Vorontsov, A. V. (2019). Advancing Fenton and photo-Fenton water treatment through the catalyst design. Journal of Hazardous Materials, 372, 103-112.